Spin-transfer torque and current-induced vortex superlattices in nanomagnets

Oleksii M. Volkov,[1] Volodymyr P. Kravchuk,[2,*] Denis D. Sheka,[1,2] and Yuri Gaididei[2]

[1]*Taras Shevchenko National University of Kiev, 01601 Kiev, Ukraine*
[2]*Institute for Theoretical Physics, 03143 Kiev, Ukraine*

Influence of the spin-transfer torque on the vortex state magnetic nanodisk is studied numerically via the Slonczewski-Berger mechanism. The existence of a critical current is determined for the case of same-directed electrical current, its spin polarization, and the polarity of the vortex. The critical current separates two regimes: (i) deformed but *static* vortex state and (ii) essentially *dynamic* state under which the spatiotemporal periodic structures can appear. The structure is a stable vortex-antivortex lattice. Symmetry of the lattice depends on the applied current value, and for high currents (close to saturation) only square lattices are observed. General relations for size of the stable lattice are obtained analytically.

Vortices are ubiquitous in nature. They play a fundamental role in various physical systems, and one of their fascinating features is the possibility of creating a variety of periodic structures. Examples are fluids,[1] superconductors of type II where vortices and vortex lattices are created under the action of magnetic field,[2] vortices and their arrays nucleate in rotating superfluid helium,[3] and Bose-Einstein condensates (BECs).[4] Lattices of topologically nontrivial structures (skyrmions) were also observed recently in weak ferromagnets.[5,6] Submicron-size magnetic planar structures give another example where the vortices play a crucial role. These structures, due to interplay between short-range exchange interaction and long-range dipole interaction, have a curling ground state.[7] One way to control the behavior of nanomagnets is to pass a spin-polarized current through the nanodot. As was discovered by Slonczewski[8] and Berger,[9] the spin-polarized current acts as an effective spin torque, which is an important feature for design of electrically controlled devices in spintronics.[10]

It was shown theoretically[11–13] and experimentally[14] that the dc spin-polarized current passing perpendicularly to the nanodisk can excite the circular motion of the vortex core. Such a circular motion can be excited[11] under two conditions: the current density $|j|$ exceeds some critical value j_c and $j\sigma p < 0$, where $\sigma = \pm 1$ is direction of spin polarization of the current (along the normal to the nanodisk $\hat{z}$) and $p = \pm 1$ is the vortex polarity (the direction of the vortex core magnetization). When $j\sigma p > 0$, the vortex core remains at the center of the disk.

The aim of this Brief Report is to show that passing the spin-polarized electrical current with $j\sigma p > 0$ through magnetic nanodisks can lead to creation of *periodic vortex-antivortex arrays*. This is a phenomenon with a threshold: It occurs when the current density exceeds some critical value which depends on material parameters of the nanomagnet and its sizes. We report about numerical investigation of the influence of the spin-polarized current on a vortex state nanodisk for a wide range of current densities. Our micromagnetic simulations[15] are based on the Landau-Lifshitz-Slonczewski equation[8,9,16]:

$$\dot{\boldsymbol{m}} = \boldsymbol{m} \times \delta\mathcal{E}/\delta\boldsymbol{m} + \alpha[\boldsymbol{m} \times \dot{\boldsymbol{m}}] - \sigma j \varepsilon \boldsymbol{m} \times [\boldsymbol{m} \times \hat{\boldsymbol{z}}]. \quad (1)$$

Here $\boldsymbol{m} = (\sin\theta\cos\phi, \sin\theta\sin\phi, \cos\theta)$ is a normalized magnetization, the overdot indicates a derivative with respect to the

rescaled time in units of $(4\pi\gamma M_s)^{-1}$, γ is the gyromagnetic ratio, M_s is the saturation magnetization, and $\mathcal{E} = E/(4\pi M_s^2)$ is the normalized magnetic energy. The normalized electrical current density $j = J/J_0$, where $J_0 = M_s^2 |e|h/\hbar$, with e being the electron charge, h being the sample thickness, and $\hbar$ being the Planck constant. Here and below it is assumed that the current flow and its spin polarization are directed along the $\hat{z}$ axis. The spin-transfer torque efficiency function ε has the form $\varepsilon = \eta\Lambda^2/[(\Lambda^2 + 1) + (\Lambda^2 - 1)\sigma(\boldsymbol{m} \cdot \hat{\boldsymbol{z}})]$, where η is the degree of spin polarization and parameter Λ describes the mismatch between spacer and ferromagnet resistance.[16,17] It should be noted that Eq. (1) is appropriate for magnets which are magnetized uniformly along the current flow. Therefore, we restrict ourself to the relatively thin samples ($h \leqslant 20$ nm) with assumption that their magnetization is uniform along the $\hat{z}$ axis.

By studying the response of the vortex state to the spin-transfer torque, one can distinguish two critical current densities: j_1 and j_2. When $j < j_1$, the stationary state of the system is a deformed vortex state (see below). When $j > j_2$, the system goes in a saturated state when all spins are aligned along the $\hat{z}$ axis. When $j_1 < j < j_2$, a rich variety of dynamic states is observed: The system demonstrates either chaotic dynamics of vortex-antivortex two-dimensional (2D) gas or regular and stable vortex-antivortex lattices.

In the no-driving case, the ground state of the nanodot is a vortex state with $\cos\theta_v = pf(r)$ where an exponentially localized function $f(r)$ describes the vortex core profile, and $\phi_v = \chi \pm \pi/2$ with (r, χ) being polar coordinates originated in the disk center. First of all, we studied how the ground vortex state θ_v, ϕ_v is modified under an influence of the spin-polarized current. Starting from the current $j = 0$, we increased j step by step with full relaxation on each step and with size of the step $\Delta j \ll j_1$. A typical deformed vortex state is shown in the lower inset of the Fig. 1. Changes of the out-of-plane component of the vortex distribution are negligibly small ($\theta \approx \theta_v$), while the in-plane structure is deformed appreciably and can be described as $\phi = \phi_v + \psi(r)$. The deformation ψ is a nonmonotonic function of r. Its amplitude is an increasing function of the current strength j. The presence of the deformation function $\psi(r)$ means an appearance of volume magnetostatic charges and an increase of the corresponding magnetostatic energy. As a result, at $j = j_1$, the vortex at the
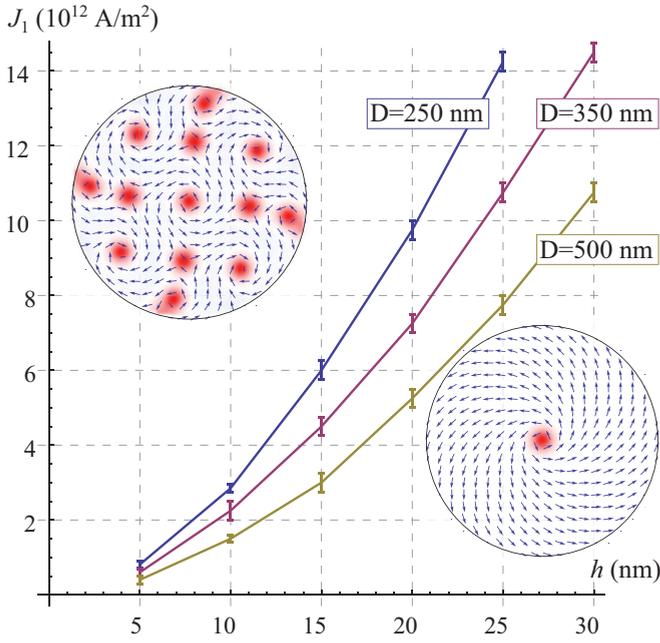
FIG. 1. (Color online) Dependence of critical current J_1 on the nanodisk thickness for different disk diameters. Insets show magnetization structures in nanodisk with $D = 250$ nm and $h = 15$ nm for different current densities: $J = 5.75 \times 10^{12}$ $A/m^2 \lesssim J_1$ (bottom right inset), $J = 6 \times 10^{12}$ $A/m^2 \gtrsim J_1$ (upper left inset).

center of disk ceases to be a stable stationary state. The vortex escapes from the disk center, moving in a spiral trajectory.

The critical current j_1 is an increasing function of the disk thickness (see Fig. 1). This fact emphasizes the important role of the volume magnetostatic charges in the phenomenon. The mentioned spiral vortex motion is accompanied by intensive generation of the magnons and results in the appearance of a gas of vortex-antivortex pairs. As a rule, the motion vortices in this state are quite irregular. However, for some values of the current in the range (j_1, j_2), instead of chaotic gaslike dynamics, stable spatially regular vortex-antivortex structures appear (as an example, see the upper inset of the Fig. 1). The following part of this Brief Report is devoted to studying this phenomenon.

To study the observed superstructures in detail, we used two methods: (i) the spin current of the certain density is sharply applied to the vortex state nanodisk and (ii) the nanodisk is previously saturated to the uniform state by a strong external magnetic field which is applied perpendicularly to the disk plane, the current of necessary density is switched on, and the external field is adiabatically diminished down to zero: $\boldsymbol{B} = e^{-t/\tau}[B_0\hat{\boldsymbol{z}} + \boldsymbol{b}(\boldsymbol{r},t)],$[18] where B_0 is saturation field, the time parameter τ is much greater than the typical time of spin wave dissipation, and an additional field $\boldsymbol{b}$ with $|\boldsymbol{b}| \ll B_0$ was added to avoid instable equilibrium states.

Possible vortex-antivortex structures which appear for $j_1 < j < j_2$ are classified and shown in Fig. 2. The obtained current diagram has the following properties: (i) The regular structures appear in the vicinity of the critical currents j_1 and j_2. (ii) The regions where the regular structures exist become wider with increasing disk thickness and these regions vanish for thin disks. (iii) Regular structures have a well-pronounced
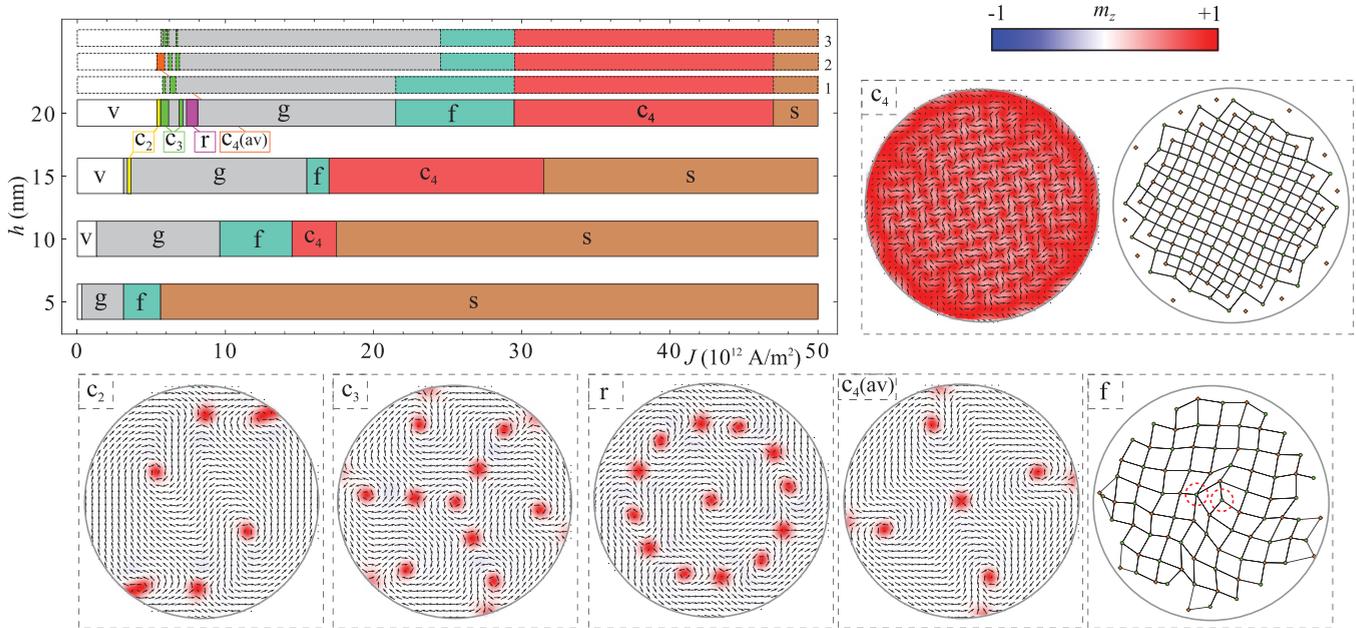

FIG. 2. (Color online) The current diagrams of periodic structures in the nanodisk with diameter $D = 350$ nm for thicknesses $h = 5, 10, 15,$ and 20 nm. The data are obtained using numerical simulations by method (ii); see text. For $h = 20$ nm, three additional diagrams were obtained: (1) method (i), (2) method (ii) with zero damping ($\alpha = 0$), and (3) method (i) with $\alpha = 0$. The obtained states are classified in the following groups: (v) static deformed vortex state, (g) regime of the chaotic dynamics of the vortex-antivortex gas, (f) fluid-like dynamics (see text), and (s) saturation along the current direction. The other states are illustrated in the insets: arrows show the in-plane magnetization distribution, and the out-of-plane component is shown by color (grayscale). The right part of the inset (c_4) and inset (f) present the vortex-antivortex lattices: Vortices are shown by circles and antivortices are shown by diamonds. All presented insets are obtained for thickness $h = 20$ nm and for the following currents (in units of 10^{12} A/m^2): (c_2) 5.5, (c_3) 7, (r) 8, (c_4) 36, [c_4 (av)] 5.5 for $\alpha = 0$, and (f) 24.
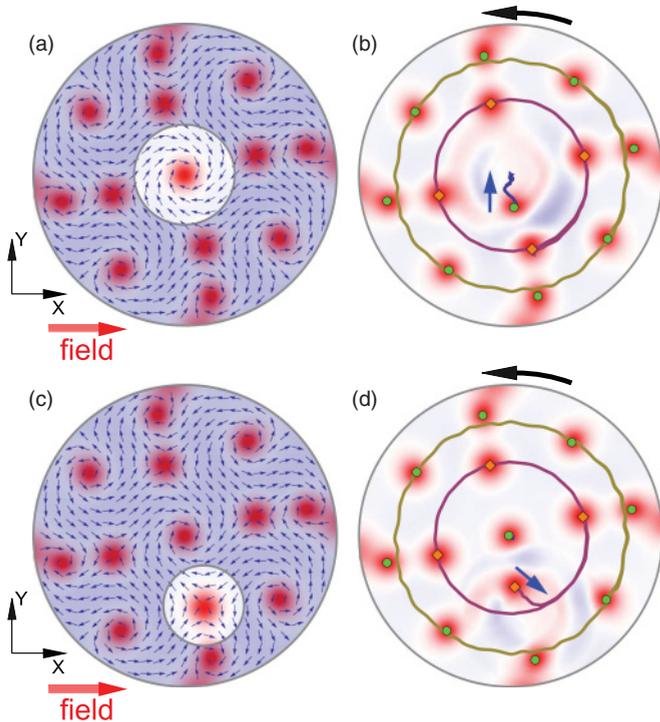
FIG. 3. (Color online) Stability of the periodic structure in nanodisk with $D = 250$ nm and $h = 20$ nm. The upper row illustrates the stability of the central vortex, and the lower row shows the antivortex. Left column: the fixed (dark) and free (bright) magnetization distribution. The field pulse (arrow in the lower left) with the amplitude increasing up to 150 mT was applied inside a free area during $t = 0.75$ ns in order to shift (a) vortex or (c) antivortex. Right column: trajectories of the shifted vortex (antivortex) and its neighbors. The curved arrow on the top indicates the rotating direction of the structure.

symmetry: A system with rotary-reflection(S_2) symmetry and systems with rotational $C_n(n = 3,4,6)$ symmetry were observed. They rotate bodily around the disk center with frequencies much lower then the corresponding gyrofrequency of the free vortex. The magnitude of the rotation frequency and its sign depend on the current. (iv) The structures become more compact with increasing current. (v) For the currents close to j_2, a crystal-like structure with a square lattice appears. (vi) As the current decreases, line defects appear in such vortex-antivortex crystals; see inset (f) of Fig. 2 (the defects are surrounded by dashed circles). As a result, the crystal loses the long-range symmetry but a short-range order is preserved: Each vortex has four nearest neighbor antivortices and vice versa. The defects permanently move within the structure, and the whole dynamics is similar to the dynamics in fluids. (vii) Further decrease of the current destroys the short-range order in the system and a vortex-antivortex gas phase appears.

It is important to note that the crystal-like structures appear in current driven nanodots even in the no-damping case ($\alpha = 0$), and the interval of their existence only weakly depends on the damping coefficient α and does not depend on the method of structure creation. In contrast to this, the thresholds and the intervals of existence of regular structures with a few vortex-antivortex pairs depend both on the damping

coefficient and on the method of generation. These regular structures exist also in the no-damping case.

The total vorticity $q = \sum_{k=1}^{N} q_k$, where N is the total number of the particles [vortices (the winding number $q_k = +1$) and antivortices ($q_k = -1$)], is the same for all regular structures and it is equal to $+1$ (as for the single vortex). The structures with a few vortex-antivortex pairs also have $q = 1$ if one takes into account edge solitons. The edge soliton (boojum[19]) is a half of an antivortex which moves on the disk edge, and it has the winding number $q_k = -1/2$. Each of mentioned regular vortex-antivortex structures represents a stationary state of the system. It means that the energy $\mathcal{E}$ and the total momentum[20] $\mathcal{J} = \int (\cos\theta - 1)(1 - \partial_\chi \phi) d\mathbf{r}$ must be time independent. Considering the most intriguing no-damping case, one can obtain from Eqs. (1) that

$$\dot{\mathcal{E}} = -\sigma j \int \varepsilon \sin^2\theta \, \dot{\phi} \, d\mathbf{r},$$

$$\dot{\mathcal{J}} = \sigma j \int \varepsilon \sin^2\theta (1 - \partial_\chi \phi) d\mathbf{r}. \qquad (2)$$

To describe the multiple vortex-antivortex structure, the following ansatz can be used:

$$\cos\theta = \sum_{k=1}^{N} f(|z - Z_k|), \quad \phi = \sum_{k=1}^{N} q_k \arg(z - Z_k), \qquad (3)$$

where $z = re^{i\chi}$ and $Z_k = R_k e^{i\Phi_k}$ with (R_k, Φ_k) being polar coordinates of the kth particle. Substituting (3) into the expressions (2) and assuming that total area of the particles cores is much smaller than the disk area $\mathcal{S}$, one can obtain

$$\dot{\mathcal{J}} \approx -\sigma j \xi \mathcal{J}, \quad \mathcal{J} \approx \pi h \sum_k q_k R_k^2 + \mathcal{S}h\left(1 - \sum_k q_k\right)$$

$$\dot{\mathcal{E}} \approx -\pi h \sigma j \xi \sum_k q_k R_k^2 \dot{\Phi}_k, \qquad (4)$$

where $\xi = \eta \Lambda^2 / (\Lambda^2 + 1)$. Thus the stationarity conditions $\dot{\mathcal{E}} = 0$ and $\dot{\mathcal{J}} = 0$ can be satisfied if

$$q \equiv \sum_{k=1}^{N} q_k = 1, \quad \sum_k q_k R_k^2 = 0, \quad \dot{\Phi}_k = \Omega = \text{const.} \qquad (5)$$

Moreover, in the process of the structure formation $\mathcal{J} = \mathcal{J}_0 \exp(-t/t_0)$, where $t_0 = (\sigma \xi j)^{-1}$ is typical time of the formation, and systems with total vorticity $q = 1$ have linear dependence between energy and momentum, $\mathcal{E} = \Omega \mathcal{J}$. For all regular structures obtained in the simulations $\sum_k q_k = 1$ (taking into account edge solitons), $\dot{\Phi}_k = \text{const}$, and $|\sum_k q_k (R_k/L)^2| \lesssim 10^{-2}$ with L being the disk radius.

To validate our analytical considerations, we carried out a direct stability check. To this end we first applied the field pulse in the disk plane [arrow in lower left of Figs. 3(a) and 3(c)], which was spatially localized nearby the central vortex in a circular region with a radius of 50 nm, keeping the rest of the magnetization distribution artificially fixed during the field pulse time; see Fig. 3(a). Such a field pulse shifts a vortex perpendicular to the field direction. After the pulse was switched off the spin-current-induced magnetization dynamics was simulated as usual. We found that the vortex was turned back to its origin in a short time (about 60 ps)

and a whole structure continued its rotation; see Fig. 3(b). Something similar takes place for the antivortex stability [cf. Figs. 3(c) and 3(d)]. We conclude that the superstructure is locally stable: Only the strong field pulse can destroy the structure.

In conclusion, we predicted and studied numerically the spatially periodic vortex-antivortex structures which appear in nanomagnets under the influence of spin-transfer torque. The structure formation is only weekly influenced by Gilbert damping,[21] and it results from effective dissipation induced by the spin current. Furthermore, we obtain the compact periodic structures [see inset (c_4) of the Fig. 2] in square-shaped nanodots with sizes and currents being the same as for the nanodisks. We demonstrated analytically and confirmed numerically fulfillment of conditions (5) for the periodic structures.

*vkravchuk@bitp.kiev.ua

[1] W. Thomson, *Mathematical and Physical Papers*, Hydrodynamics and General Dynamics, Vol. 4 (Cambridge University Press, Cambridge, 1910), p. 563.

[2] A. A. Abrikosov, Rev. Mod. Phys. **76**, 975 (2004).

[3] R. J. Donnelly, *Quantized Vortices in Helium II*, Cambridge Studies in Low Temperature Physics, Vol. 3 (Cambridge University Press, Cambridge, 1991), p. 346.

[4] A. L. Fetter, Rev. Mod. Phys. **81**, 647 (2009).

[5] S. Mühlbauer, B. Binz, F. Jonietz, C. Pfleiderer, A. Rosch, A. Neubauer, R. Georgii, and P. Böni, Science **323**, 915 (2009).

[6] X. Z. Yu, Y. Onose, N. Kanazawa, J. H. Park, J. H. Han, Y. Matsui, N. Nagaosa, and T. Y., Nature Lett. **465**, 901 (2010).

[7] N. A. Usov and S. E. Peschany, J. Magn. Magn. Mater. **118**, L290 (1993).

[8] J. C. Slonczewski, J. Magn. Magn. Mater. **159**, L1 (1996).

[9] L. Berger, Phys. Rev. B **54**, 9353 (1996).

[10] I. Zutic, J. Fabian, and S. D. Sarma, Rev. Mod. Phys. **76**, 323 (2004); Y. Tserkovnyak, A. Brataas, G. E. W. Bauer, and B. I. Halperin, *ibid.* **77**, 1375 (2005).

[11] J.-G. Caputo, Y. Gaididei, F. G. Mertens, and D. D. Sheka, Phys. Rev. Lett. **98**, 056604 (2007); D. D. Sheka, Y. Gaididei, and F. G. Mertens, Appl. Phys. Lett. **91**, 082509 (2007); Y. Gaididei, V. P. Kravchuk, and D. D. Sheka, Int. J. Quantum Chem. **110**, 83 (2010).

[12] B. A. Ivanov and C. E. Zaspel, Phys. Rev. Lett. **99**, 247208 (2007).

[13] Y.-S. Choi, M.-W. Yoo, K.-S. Lee, Y.-S. Yu, H. Jung, and S.-K. Kim, Appl. Phys. Lett. **96**, 072507 (2010).

[14] V. S. Pribiag, I. N. Krivorotov, G. D. Fuchs, P. M. Braganca, O. Ozatay, J. C. Sankey, D. C. Ralph, and R. A. Buhrman, Nat. Phys. **3**, 498 (2007).

[15] We used the OOMMF code, version 1.2a4 [http://math.nist.gov/oommf/]. All simulations were performed for material parameters of permalloy: exchange constant $A = 1.3 \times 10^{-11}$ J/m, saturation magnetization $M_s = 8.6 \times 10^5 A/m$, the anisotropy was neglected, and damping was chosen close to natural value $\alpha = 0.01$ (with the exception of some cases mentioned in the text with $\alpha = 0$). The mesh cell was chosen to be $3 \times 3 \times h$ nm. The current parameters $\sigma = +1$, $\eta = 0.4$, and $\Lambda = 2$ were the same for all simulations.

[16] J. C. Slonczewski, J. Magn. Magn. Mater. **247**, 324 (2002).

[17] V. Sluka, A. Kakay, A. Deac, D. Buergler, R. Hertel, and C. Schneider, e-print arXiv:1010.4791.

[18] $B_0 = 1.1$ T, $\tau = 5$ ns, $\boldsymbol{b} = b_0 \cos\omega t (\cos\chi, \sin\chi, 0)$, where $b_0 = 0.01$ T, and frequency $\omega = 50$ GHz is much greater then typical eigenfrequencies of magnon modes in the disks of the considered sizes.

[19] G. Volovik, *The Universe in a Helium Droplet* (Oxford University Press, Oxford, 2003).

[20] Y. Gaididei, V. P. Kravchuk, D. D. Sheka, and F. G. Mertens, Phys. Rev. B **81**, 094431 (2010).

[21] The formation of vortex-antivortex patterns was confirmed also by spin-lattice simulations with nominal damping constant and without damping term in the disk- and square-shaped samples.

[22] Kyiv National Taras Shevchenko University high-performance computing cluster: [http://cluster.univ.kiev.ua/eng/about].